Scientific Research Publishing

Journal of Transportation Technologies, 2026, 16(1), 18-37
https://www.scirp.org/journal/jtts
ISSN Online: 2160-0481
ISSN Print: 2160-0473

Impact of Sinusoidal Speed Humps on the Dynamics and Comfort of Electric-Assisted Child-Carrying Bicycles

Sajith Udayanga*, Aya Kojima, Hisashi Kubota

Graduate School of Science and Engineering, Saitama University, Saitama, Japan
Email: *pathiraja.a.s.u.605@ms.saitama-u.ac.jp, akojima@mail.saitama-u.ac.jp, hisashi@mail.saitama-u.ac.jp

How to cite this paper: Udayanga, S., Kojima, A. and Kubota, H. (2026) Impact of Sinusoidal Speed Humps on the Dynamics and Comfort of Electric-Assisted Child-Carrying Bicycles. *Journal of Transportation Technologies*, **16**, 18-37.
https://doi.org/10.4236/jtts.2026.161002

Received: October 14, 2025
Accepted: November 23, 2025
Published: November 26, 2025

Abstract

The rapid growth of electric-assisted child-carrying bicycles in urban areas marks the need to evaluate passenger comfort when traversing traffic-calming devices. This study compares vibration exposure on sinusoidal speed humps and conventional speed bumps in Japanese Zone 30+ areas. A controlled experiment used triaxial accelerometers at three bicycle locations (front child seat, frame center, rear child seat) across 144 scenarios combining two-wheel sizes (20-inch, 26-inch), three loading conditions (unladen, 12 kg front load, 12 kg rear load), and four speeds (5 to 20 km/h). Acceleration signals sampled at 50-millisecond intervals were analyzed using the Dynamic Comfort Index (DCI) and ISO 2631-1 metrics: Root Mean Square acceleration (RMS), Vibration Dose Value (VDV), and crest factor. Sinusoidal profiles produced DCI distributions closely aligned with smooth-road benchmarks within 5% of baseline comfort whereas conventional bumps produced DCI values deviating up to 25%. Results show that sinusoidal humps significantly reduce peak and cumulative vibration across all configurations, with the greatest improvement at the front child seat. Sinusoidal hump profiles obtained comfort levels within acceptable thresholds even at higher speeds typical of electric assist, whereas conventional bumps often exceeded discomfort limits. These findings support adopting sinusoidal speed humps in school zones to balance effective speed control with child passenger comfort and safety in sustainable transportation systems.

Keywords

Child-Carrying Bicycles, Speed Humps, Traffic Calming, Vibration Analysis, Comfort Assessment, Zone 30+

1. Introduction

Urban families in Japan increasingly rely on electric-assisted child-carrying bicycles commonly called Mama Chari to navigate dense city streets, avoid high vehicle ownership costs, and manage limited parking. Narrow residential streets further encourage bicycle use over automobiles, while electric-assist technology enhances pedal efficiency (maintain speeds of 20 - 25 km/h with minimum effort) and riding pleasure, enabling longer trips and reducing physical exertion for adult riders. Consequently, Mama Chari has become integral to daily routines such as school commutes, grocery shopping, and family outings [1].

The Zone 30+ concept, expanding the standard 30 km/h speed limit zones to include additional traffic calming devices, has gained traction in Japanese municipalities, particularly around school environments. Implementation often involves installing speed humps, flat-top tables, and raised crosswalks to protect vulnerable road users. While these measures effectively reduce traffic speeds, they also introduce frequent interactions between child-carrying bicycles and physical calming devices, potentially subjecting infant passengers to repeated shock and vibration events [2]. **Figure 1** shows the sinusoidal speed hump utilized for the experiment. The portable sinusoidal rubber hump (Flexitec®) installed inside the institutional road has been used to conduct the experiment.

Figure 1. Sinusoidal speed hump used for the experiment.

The Flexitec® portable speed hump constitutes a paradigmatic advancement in modular traffic-calming infrastructure, developed through systematic collaborative research between Saitama University and Nippon Liner Co., Ltd. as an experimental "sinusoidal mobile hump" deployment system. This technological innovation employs discrete one-meter square elastomeric modules that facilitate rapid iterative installation and spatial reconfiguration without permanent road surface modification, thereby enabling empirical optimization of geometric parameters and inter-unit spacing configurations in controlled experimental environments. The system's sinusoidal profile geometry represents a deliberate depar-

ture from conventional parabolic or flat-top designs, incorporating mathematically continuous curvature transitions that minimize impulsive vertical accelerations and associated noise generation addressing Japan's stringent regulatory frameworks governing traffic-induced environmental disturbances in high-density residential zones. Figure 2 illustrates the conventional asphalt made speed bump used as a control condition of the experiment.

Figure 2. Conventional asphalt made speed bump.

In Japanese urban districts, early traffic calming schemes implemented trapezoidal speed humps 100 mm high with 1.5 m bases to enforce 30 km/h limits. While effective for motor vehicles, these profiles produced harsh decelerations (>3 m/s^2) and transmitted severe shocks to two-wheeled traffic, including child-carrying cargo bikes and electric-assist "Mama Chari", leading to rider discomfort and accelerated equipment wear. Subsequent evaluations identified that sinusoidal humps half-sine waveforms spanning 3 m with 75 mm crest height could maintain speed reduction efficacy while attenuating peak accelerations by up to 30% for bicycles at 15 km/h, thereby enhancing rider comfort without compromising safety. In 2011, these findings informed national design standards for Zone 30+ installations in school zones, prescribing 20 to 40 mm crest tolerances and extended crest lengths; field implementations reported average Mama Chari speeds of 18 km/h and peak vertical accelerations below 3 m/s^2, markedly improving child-seat comfort and reducing rider fatigue [3].

Electric-assist bicycles can achieve sustained speeds of 20 - 25 km/h with minimal rider effort, substantially higher than typical conventional bicycle speeds of 10 - 15 km/h. When traversing speed humps at these increased velocities, Mama Chari transmits elevated shock magnitudes and continuous vibration to child seats, thereby heightening the risk of discomfort or injury for young passengers. Accurate characterization of mitigation conditions is essential for designing child seats and traffic calming infrastructure that mitigate adverse shock exposures [4]. Figure 3 shows the electric assisted bicycles mobilized for the experiment.

20” Wheel Size Bicycle	26” Wheel Size Bicycle

Figure 3. Electric assisted bicycles mobilized for the experiment.

Electric-assist bicycles equipped with 20-inch wheels exhibit higher acceleration responsiveness and lower rotational inertia, resulting in more rapid torque transfer to the ground during start-stop urban riding, whereas 26-inch wheels demonstrate superior bump-negotiation and momentum retention due to their larger rolling radius and increased gyroscopic stability.

From a vibration standpoint, 26-inch wheels tend to attenuate road irregularities more effectively by shifting predominant excitation frequencies toward the lower end of the spectrum and reducing high-frequency vertical inputs transmitted to the frame and cargo platform; by contrast, 20-inch wheels, with their smaller diameter and quicker angular displacement, produce higher-frequency vibration components that can increase comfort challenges for child passengers unless mitigated by suspension or tire pressure adjustments. Consequently, wheel-size selection in Japanese electric-assist child-carrying bicycles compromise between agile acceleration and vibration comfort, informing design decisions for payload-sensitive applications.

2. Literature Review

Investigations into passenger comfort provide a valuable foundation for examining road-induced vibrations affecting infant passengers [5]. On bicycles, comfort is influenced by both mechanical factors such as bicycle and component design and environmental conditions, including weather, route geometry, and road surface roughness. Human comfort further depends on biomechanical factors (whole-body vibration exposure, body dynamics, and kinematics) and physiological characteristics (e.g., body size, weight, and sex).

Although extensive research has addressed how environmental variables like irregular pavement and weather impact adult cyclists' comfort, there remains a scarcity of studies focusing on the biomechanical and physiological dimensions of comfort for infants or young children riding in bicycle seats, cargo bikes, or trailers.

2.1. Child-Carrying Bicycle Vibration and Acceleration

Literature on child-carrying bicycle vibration and comfort presents a rapidly expanding field of inquiry, primarily driven by increasing adoption of sustainable family transportation systems. International research demonstrates consistently

elevated vibration exposures for child passengers compared to adult occupants in motorized vehicles, raising significant comfort and safety concerns. Comfort assessments of bicycle trailers report weighted accelerations of 1 - 3 m/s^2 on asphalt and 3 - 5 m/s^2 on cobblestone surfaces, substantially exceeding passenger-car vibration levels [6].

Comparative studies using cargo tricycles corroborate these findings, revealing dominant frequency content in the 3 - 5 Hz range, coinciding with infant head resonance frequencies and amplifying discomfort. Surface characteristics emerge as the primary determinant of exposure, with cobblestones producing threefold higher weighted accelerations than smooth asphalt at equivalent speeds. Investigations into passenger mass effects indicate that lighter dummy loads (5 kg) experience 20% higher vibration levels than heavier loads (10 kg), while tire pressure and loading variations yield minimal mitigation benefits.

The most comprehensive analyses to date document seat-pan accelerations ranging from 0.4 - 10.7 m/s^2 in cargo bicycles at 12 - 25 km/h, demonstrating that modern cargo bicycle designs often transmit shock magnitudes that exceed health risk thresholds established for adult workers. Historical stroller designs with advanced suspension outperformed contemporary models, underscoring design tradeoffs favoring weight reduction over comfort. Biomechanical testing identifies critical frequencies of 1 - 2 Hz where infant head and chest regions exhibit peak vibrational responses, suggesting potential resonance amplification during cycling operations.

2.2. Electric-Assisted Bicycle Usage in Japan

Japan's "Mama Chari" electric-assisted child-carrying bicycles have revolutionized urban family mobility. Market data show annual sales exceeding 500,000 units with 90% market penetration, reflecting their integration into daily life for errands, school commutes, and short trips. Economic factors such as high vehicle ownership costs, limited urban parking, and narrow residential streets drive Mama Chari adoption as cost-effective car alternatives. Electric-assist capabilities allow sustained speeds of 20 - 25 km/h with minimal exertion, more than doubling conventional bicycle speeds of 10 - 15 km/h. Leading manufacturers Panasonic, Bridgestone, Yamaha offer child-specific models featuring reinforced frames, stable kickstands, and reliable brakes to meet government certification requirements. Regulatory standards mandate structural integrity, heavy-duty racks, and prominent safety labels, ensuring consistent product quality and passenger protection. Research into multimodal commuting demonstrates that Mama Chari facilitates first-mile connectivity to public transit, extending daily trip ranges while reducing physical strain, thereby broadening cycling demographics beyond enthusiasts to include families and older adults [7].

2.3. Zone 30+ Implementation in Japan

The Zone 30 policy, introduced nationally in September 2011, represents a paradigm shift in Japan's traffic-calming strategies. Unlike earlier schemes such as

school, silver, and community zones which imposed speed limits selectively and required complex designation procedures, Zone 30 applies a uniform 30 km/h speed limit across residential street networks without minimum area thresholds. This policy leverages a combination of regulatory measures (speed signage and road markings) and optional physical treatments (e.g., road humps, mini roundabouts) to achieve consistent speed reduction. A multicenter evaluation of 3105 Zone 30 areas demonstrated a significant 22% decrease in mean vehicle speeds and a 15% reduction in pedestrian-related crashes over five years, emphasizing their efficacy in enhancing safety and environmental quality. Early efforts (School Zones, Neighborhood Zones, Community Zones) achieved only 8.0% injury reduction on narrow roads, compared to 29.2% on arterial roads between 2000 - 2010. Zone 30+ removed complex implementation burdens, enabling rapid deployment of speed limits supplemented by signage, navigation integration, and infrastructure modifications [8].

Building on Zone 30's success, the Zone 30+ program was piloted in Tokyo's Sumida Ward on March 24, 2023, integrating mandatory speed limits with targeted infrastructure interventions. Zone 30+ employs site-specific combinations of slalom-type chicanes, neckdowns (narrowed curb extensions), vertical deflections (speed humps), bollard installations, and high-visibility wayfinding markings. A quasi-experimental study comparing treatment and control segments found a 30% greater reduction in 85th-percentile speeds within Zone 30+ areas and a 25% drop in near-miss incidents, indicating enhanced compliance and perceived safety among vulnerable users. Community engagement joint inspections by schools, police, and road authorities support site-specific measures such as portable speed hump trials and pedestrian crossing enhancements, ensuring sustained compliance and public acceptance [9].

2.4. Speed Humps as a Traffic Calming Device

Japan's transition from trapezoidal to sinusoidal speed-hump geometries addresses the need for effective speed control with improved bicycle comfort. Conventional trapezoidal humps (100 mm height, 1.5 m base) reduced vehicle speeds but generated harsh decelerations (>3 m/s^2) and severe shocks for two-wheeled traffic. Systematic evaluations identified half-sine sinusoidal profiles (3 m base, 75 mm height) as optimal, reducing peak accelerations by 20% to 25% for cars and up to 30% for child-carrying bicycles at 15 km/h. In 2011, national standards incorporated sinusoidal design parameters 20 to 40 mm crest tolerances and 3 m transition lengths for Zone 30+ installations [10].

Field studies in Tokyo and Osaka confirmed average cyclist speeds at 18 km/h with Mama Chari experiencing vertical accelerations below 3 m/s^2, significantly enhancing comfort compared to trapezoidal profiles. The 2023 "Mama Chari-Friendly Calming" pilot introduced modular rubber-steel composite segments with adjustable curvature, achieving an additional 10% shock reduction over concrete sinusoidal humps while maintaining speed deterrence, exemplifying Japan's

data-driven infrastructure innovation [11].

2.5. Dynamic Comfort Index

Dynamic Comfort Index (DCI) serves as an integrative metric that quantifies the cumulative vibrational exposure experienced by a rider over time, thereby offering a more holistic assessment of ride quality than instantaneous measures such as peak acceleration or root mean square (RMS) values alone. By incorporating both the magnitude and duration of vertical and lateral accelerations, DCI captures transient excitations such as those induced when traversing speed humps or uneven pavement that can significantly influence perceived comfort. For bicycle applications, DCI enables comparison across different vehicle configurations (e.g., frame stiffness, suspension design, tire pressure) and environmental conditions (e.g., surface roughness, traffic calming features) by translating complex, time-varying vibration signals into a single, comparable index. This unified approach facilitates the identification of design parameters or operational practices that minimize long-term vibrational loads on both rider and cargo, including sensitive payloads such as children.

Application of DCI in the context of electric-assisted child-carrying bicycles is particularly valuable because motor-assist behavior introduces additional dynamic forces that traditional comfort indices may overlook. Regenerative braking and torque-smoothing algorithms modulate longitudinal and vertical accelerations in real time, altering the frequency content and temporal distribution of vibrational input to the bicycle frame and cargo platform.

By integrating these effects, DCI provides a sensitive gauge for calibrating assist levels and suspension settings to mitigate potentially harmful vibration doses to young passengers. When combined with pediatric biodynamic models, DCI based evaluations can inform evidence-based guidelines for speed hump geometry and motor-control strategies that safeguard child comfort and safety without compromising the traffic calming objectives [12]. **Table 1** summarizes the significant findings of the previous studies related to dynamics of the child carrying bicycles.

Table 1. Summary of key literature findings.

Study	Details of the Study	
	Device Type	Key Finding
Behrend (1931)	Vintage stroller	Early advice warned that perambulator vibrations, despite ample suspension, were deemed uncomfortable and potentially harmful for infants [13].
Ayachi *et al.* (2015)	Adult bicycle	Identified multifaceted comfort factors; physical, biomechanical, and environmental influences on cyclist comfort [14].
Kyrollos *et al.* (2018)	Adult bicycle	Derived bicycle-specific comfort limits differing from ISO 2631-1, highlighting need for vibration guidelines suited to cyclists [15].

Continued

Rothhämel & Liu (2019)	Cycle carrier	The tyres exhibited a natural vibration frequency largely unaffected by vertical load, yet this frequency influenced the vibration patterns transmitted to the passengers [16].
Mohamed *et al.* (2019)	Electric bicycle	Speed and gradient dynamics play a crucial role in detailed cycling behavior, impacting bicycle engineering, infrastructure planning, and rider health assessments [17].
Scoz *et al.* (2021)	Adult bicycle	A bike-fit process may improve pain, discomfort and fatigue in different degrees [18].
Ahmed *et al.* (2024)	Smart bicycle	City planners should adopt innovative data-collection technologies to enhance cycling conditions [19].

3. Research Objectives

This study addresses critical knowledge gaps in understanding the vibrational dynamics and comfort implications of electric-assisted child-carrying bicycles when navigating traffic calming infrastructure in Japanese urban environments. The primary objective is to quantitatively compare vibration transmission characteristics between sinusoidal speed humps and conventional asphalt speed bumps across diverse operational parameters that reflect real-world usage patterns of Mama Chari bicycles.

- To establish empirical relationships between bicycle wheel size configurations (20-inch versus 26-inch diameter wheels) and vibration attenuation properties when traversing different speed management devices.
- To quantify the influence of payload conditions including unladen scenarios, front-seated loading (12 kg), and rear-seated loading (12 kg) on acceleration magnitudes transmitted to child seating positions.
- To characterize velocity-dependent vibration responses across the operational speed range of electric-assisted bicycles (5-20 km/h) to inform safe traversal guidelines for Zone 30+ implementations.
- To evaluate spatial distribution of vibration intensities across critical bicycle locations (front child seat, frame center, rear child seat) to identify optimal seating positions for minimizing passenger exposure.

Through systematic examination of 144 experimental scenarios, this research aims to provide quantitative foundations for sinusoidal speed hump implementation in school zones and residential areas where vulnerable road user protection remains predominant.

4. Research Methodology

A controlled factorial experimental design was implemented to systematically evaluate vibration transmission characteristics of electric-assisted child-carrying bicycles across varied operational parameters. The investigation employed two distinct bicycle configurations featuring wheel diameters of 20 inches and 26

inches, each equipped with standardized front and rear child seating attachments representative of commercially available Mama Chari models utilized in Japanese urban environments. Video footage was recorded to assist in time-referencing the vibration data. Overall research methodology shown in Figure 4 outlines the overall methodical flow of the study.

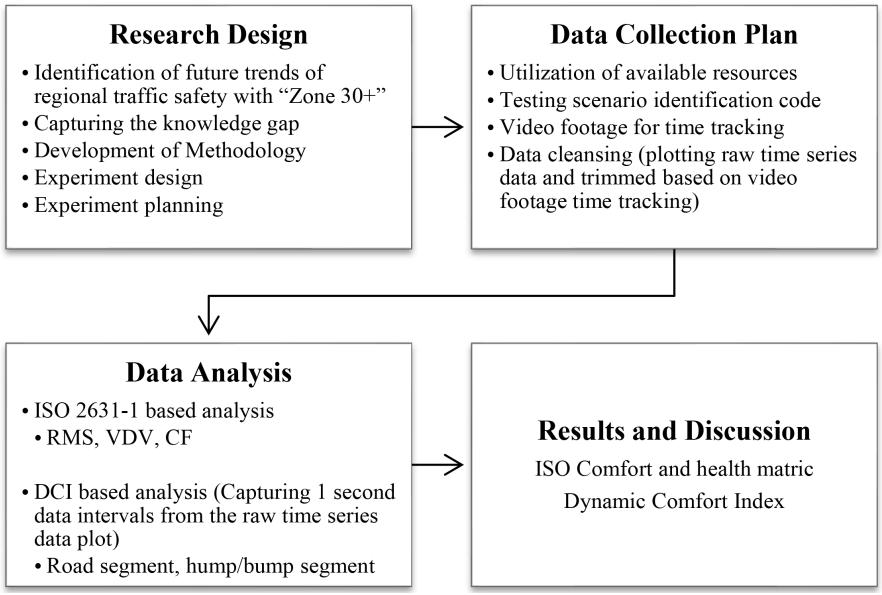

Figure 4. Sensor arrangement of the experiment.

4.1. Experiment Setup

Triaxial vibration measurements were obtained using CEM DT-178A 3-axis Vibration Dataloggers positioned at three critical locations on each bicycle configuration: the front child seat mounting point, the bicycle frame's geometric center, and the rear child seat attachment as indicated in Figure 5.

All dataloggers were horizontally oriented using integrated spirit levels to ensure consistent axis alignment, with the z-axis corresponding to vertical acceleration measurements. The instrumentation provided continuous acceleration data acquisition at 50-millisecond intervals, enabling high-resolution characterization of transient vibration events during the experiment.

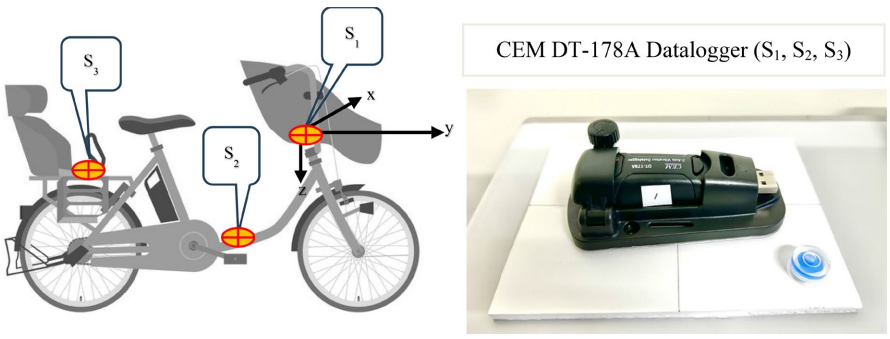

Figure 5. Sensor arrangement of the experiment.

All experimental trials were conducted by a single male rider (age 35 years, mass 65 kg, height 176 cm) with approximately ten years of cycling experience. An upright posture was maintained throughout testing using casual clothing, reflecting typical Mama Chari riding conditions in Japanese urban environments. Reporting these physical characteristics ensures experimental replicability, as rider mass and posture influence bicycle-rider system vibration response.

Two distinct traffic calming configurations served as experimental variables: conventional asphalt speed bumps representing the control condition, and portable sinusoidal speed humps constructed from modular rubber materials. The sinusoidal speed humps employed Flexitec® technology, featuring mathematically continuous curvature profiles designed to minimize impulsive vertical accelerations while maintaining effective speed reduction capabilities. The sinusoidal speed hump configuration consisted of a flat-topped design with a total base length of 6 meters. The central 2-meter section featured a flat plateau at a height of 10 cm above the road surface, while the approach and departure ramps on both sides exhibited symmetric sinusoidal profiles providing smooth transitions from the road surface to the flat top. This design follows the Flexitec® modular rubber speed hump system installed under Japan's Zone 30+ traffic calming initiatives. The conventional asphalt speed bump utilized as the control condition had a parabolic cross-sectional profile with a base width of 32 cm in the direction of travel and a maximum height of 4.5 cm at the center. This geometry represents typical non-engineered speed bumps commonly installed in Japanese institutional roadways.

4.2. Test Scenarios

Different loading scenarios were evaluated: an unladen condition, a 12 kg weight (made from box of water) placed in the front child seat, and the same weight placed in the rear child seat, as shown in Figure 6.

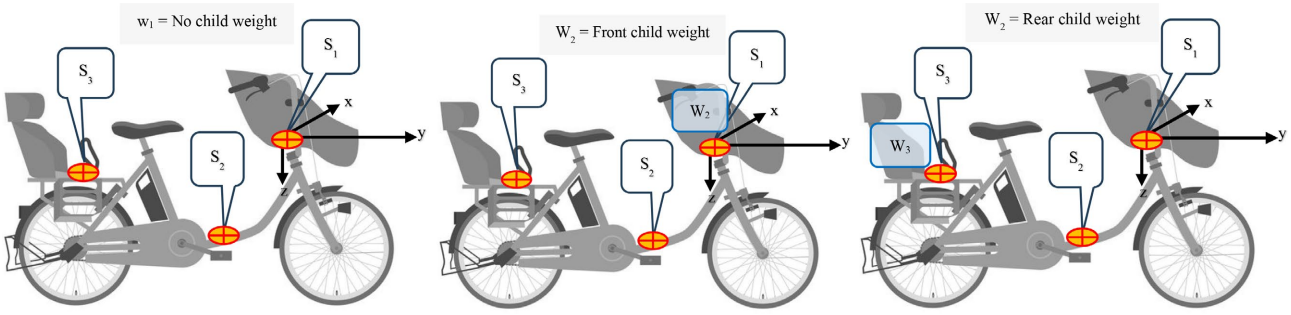

Figure 6. Different loading senarios of the experiment.

Table 2 presents the notations assigned to the test scenarios employed in this study. These symbols serve as identifiers for the variables during the data analysis process and in subsequent references throughout the study. 144 uniform data points were collected; the use of variable notations facilitated the interpretation of results and the subsequent discussion.

Table 2. Table of notations.

Notations for all test scenarios				
Load Cases	Sensors	Speeds	Hump/bump	Bicycle wheel size
W1: No child weight	S1: Front seat	5: 5 km/h		20 bike: 20-inch wheel
W2: Front child weight	S2: Frame	10: 10 km/h 15: 15 km/h	h: hump b: bump	26 bike: 26-inch wheel
W3: Rear child weight	S3: Rear seat	20: 20 km/h		

5. Data Analysis

The comprehensive experimental matrix generated 144 unique test scenarios through systematic combination of bicycle configurations (2), traffic calming devices (2), loading conditions (3), velocity parameters (4), and sensor locations (3). Maximum absolute vertical (z-axis) accelerations were extracted from each dataset to characterize peak vibration magnitudes transmitted during the experiment. Case comparable sample raw acceleration (g) versus time for two test conditions shown in Figure 7. Video footage data is used to identify the effective raw data range.

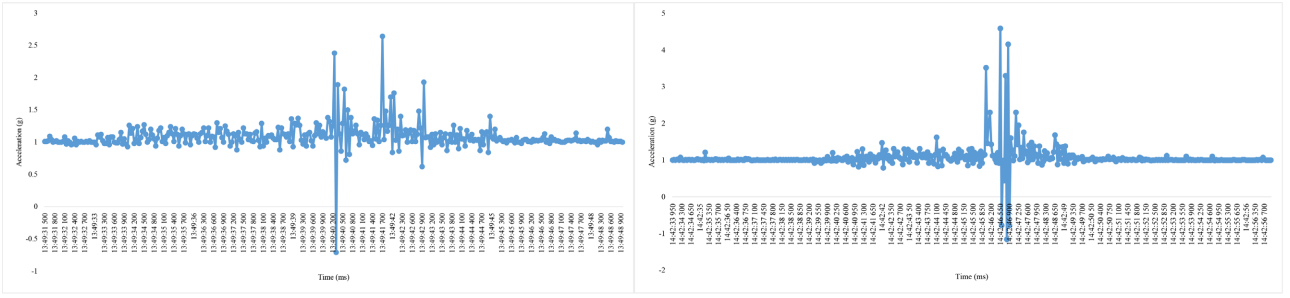

Raw vertical acceleration sample - hump

Raw vertical acceleration sample - bump

Figure 7. Sample raw acceleration (g) versus time.

5.1. Dynamic Comfort Index

The Dynamic Comfort Index (DCI) represents an exhaustive metric for evaluating the measure of comfort perceived by cyclists, incorporating a multitude of parameters. Equation (1) illustrates this index, which serves as a discrete point measurement corresponding to a one-second interval.

$$\mathrm{DCI} = \sqrt{\frac{1}{n}\sum_{i=1}^{n} a_i^2}^{-1} \tag{1}$$

In the given context, "n" denotes the quantity of observations captured within one second duration. The variable "a" signifies the vertical acceleration, quantified in meters per second squared (n = 20 samples at 50 milliseconds sampling interval). After the analysis of acceleration data, pivotal test scenarios were selected for the computation of DCI.

5.2. ISO 2631-1 Comfort and Health Indicators

ISO 2631-1 Comfort and Health Metrics for all scenarios were calculated such as RMS acceleration, Vibration Dose Value (VDV), and Crest Factor across all test scenarios. Human vibration exposure is quantified through several standardized metrics, each capturing distinct aspects of dynamic loading characteristics. For each time series RMS Acceleration (a_w) numerically calculated by discrete summation according to Equation (2) below with a unit of m/s^2. Where a_i is the i^{th} acceleration value recorded.

$$a_w = \sqrt{\frac{1}{N}\sum_{i=1}^{N}\left[a_i\right]^2} \tag{2}$$

The Vibration Dose Value (VDV) provides a fourth-power time-domain integration that is particularly sensitive to intermittent shocks and transient events, making it more appropriate for evaluating non-stationary vibration exposure where peak magnitudes may cause discomfort or injury. VDV calculated by including duration normalization multiply by $T^{(1/4)}$ if required according to the Equation (3).

$$\text{VDV} = \left(\sum_{i=1}^{N}\left[a_i\right]^4 \Delta t\right)^{1/4} \tag{3}$$

To identity the "shock" effect, spikes or impacts Crest Factor has been calculated according to the Equation (4). Where a_{peak} is the maximum absolute acceleration recorded. captures the maximum instantaneous acceleration within the measurement period, indicating the severity of individual vibration events that may exceed human tolerance thresholds.

The Crest Factor, defined as the ratio of peak to RMS acceleration, characterizes the impulsiveness of the vibration signal higher values indicating sporadic, shock-like excitations while lower values suggest more continuous, steady-state vibration patterns.

$$\text{Crest Factor} = \frac{a_{peak}}{a_w} \tag{4}$$

Although ISO 2631-1 is traditionally employed for assessing long-duration vibration exposure, its metrics can be effectively adapted to benchmark the "shock" impacts generated by traffic calming devices. As future initiatives aim to deploy multiple calming measures within school zones to enhance pedestrian and cyclist safety, a single bicycle trip may encounter several speed humps sequentially. Establishing standardized benchmarks for these transient shock events is therefore essential to inform design guidelines, optimize device spacing, and ultimately support evidence-based strategies for safer street environments.

6. Results and Discussion

Dynamic Comfort Index to provide a holistic evaluation of cyclist vibration exposure. ISO metrics (RMS, VDV, and peak acceleration) are used to classify broad comfort zones and health risk thresholds, while the DCI offers fin scale, second

by second resolution of instantaneous ride quality. Together, they reveal both cumulative vibration dose and moment to moment comfort variations: ISO measures identify sections requiring engineering intervention to meet occupational standards, whereas DCI highlights precisely where transient shocks create discomfort. This combined approach enhances the sensitivity of vibration assessments.

6.1. Results of DCI

The methodology yielded two Dynamic Comfort Index (DCI) values one for riding on a smooth road surface and one for traversing a hump. Each DCI was calculated over a one-second window of acceleration data. At low speeds, this window corresponds to relatively short distance travel, whereas at higher speeds it spans a longer segment of roadways. For hump traversal, the data window was centered on the moment of greatest impulse so that the peak acceleration impulse appears at the midpoint of the one-second interval. Results show the impact of sinusoidal speed humps on the Dynamic Comfort Index (DCI) a higher DCI indicating reduced vibration exposure and enhanced comfort experienced by child passengers on electric-assisted bicycles. Using a controlled experiment, across all 144 scenarios, encompassing two-wheel sizes (20 bike, 26 bike) evaluated against normal smooth road DCI found that sinusoidal hump performs closer to smooth road comfort levels. Both "20 bike" and "26 bike" DCI distributed closer to the smooth road DCI distribution as shown in the **Figure 8**.

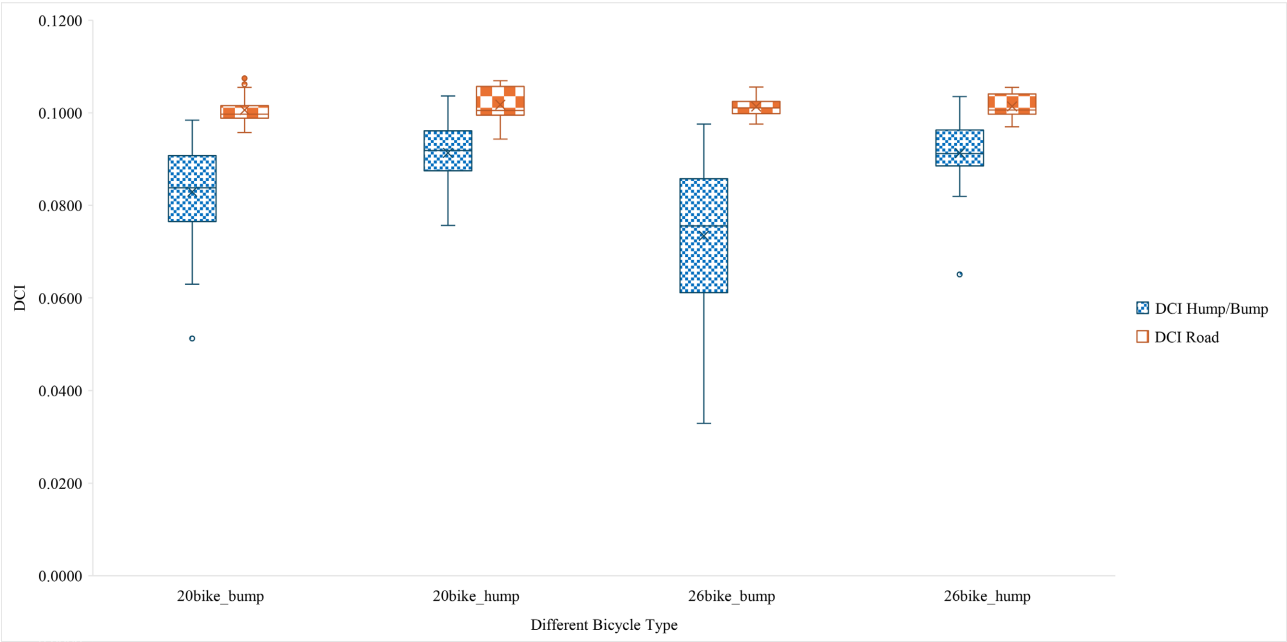

Figure 8. DCI distribution among bicycle type for all test scenarios.

6.2. Findings of ISO Comfort and Health Indicators

Analysis of absolute peak acceleration reductions across sensor locations revealed that the front-seat sensor (S1) exhibited the most pronounced attenuation under

sinusoidal humps, with a mean decrease of 29.29 m/s^2. The rear-seat sensor (S3) recorded a comparable but slightly smaller mean reduction of 27.80 m/s^2, whereas the frame-mounted sensor (S2) demonstrated a mean decrease of 21.39 m/s^2. These findings indicate that sinusoidal hump profiles confer the greatest improvement in peak vibration attenuation at the front child seat, with subsequent benefits observed at the rear seat and bicycle frame. **Figure 9** Graphically illustrates the proportionate impact of the bicycle location.

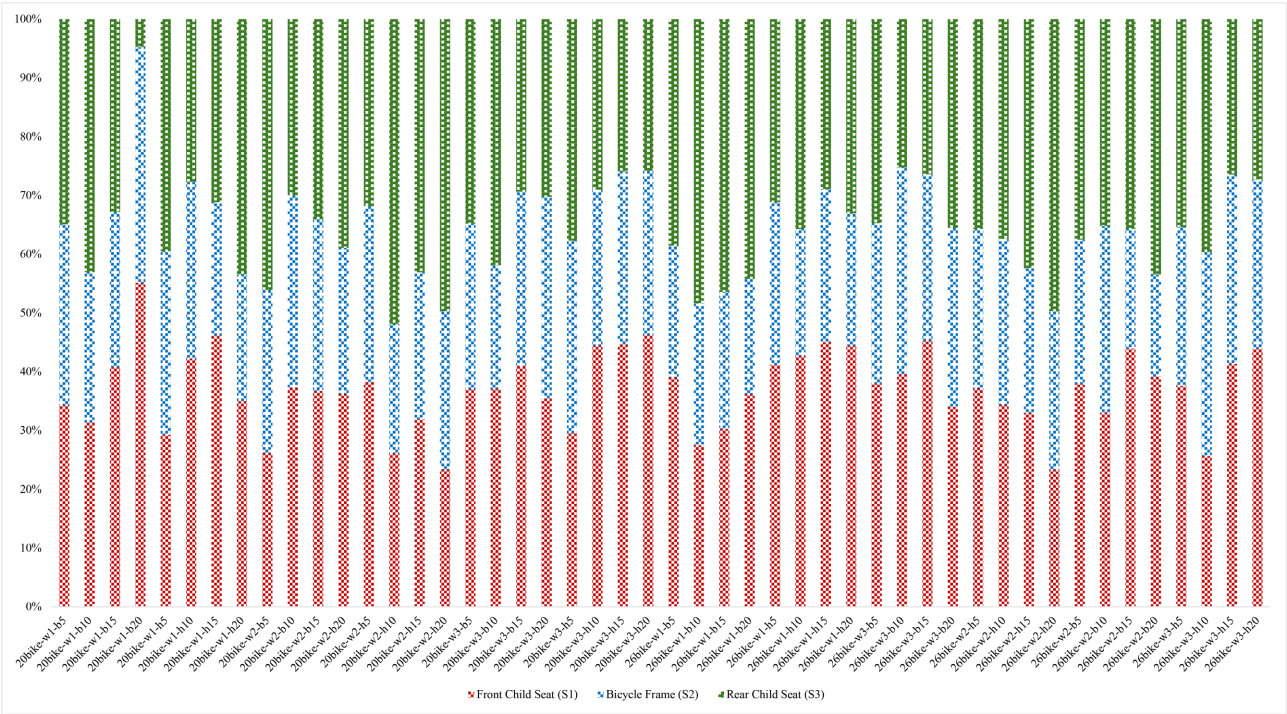

Figure 9. Absolute peak acceleration variation over bicycle location.

Examination of RMS acceleration reductions across sensor positions demonstrated that the front-seat sensor (S1) experienced the greatest mean decrease of 1.25 m/s^2 when traversing sinusoidal humps compared to conventional bumps. The rear-seat sensor (S3) recorded a moderate mean reduction of 1.09 m/s^2, while the frame-mounted sensor (S2) exhibited the smallest mean decrease of 0.91 m/s^2. These results indicate that sinusoidal hump profiles provide the most substantial RMS vibration attenuation at the front child seat location, with statistically significant but progressively smaller benefits observed at the frame and rear seat positions. **Figure 10** Graphically illustrates steady variation across all case scenarios.

Statistical comparison of VDV across sensor positions revealed that the front-seat sensor (S1) showed the largest mean reduction of 10.73 m/s$^{1.5}$ when traversing sinusoidal humps versus conventional bumps as shown in **Figure 11**. The rear-seat sensor (S3) followed with a mean decrease of 9.35 m/s$^{1.5}$, while the frame-mounted sensor (S2) exhibited a mean reduction of 5.14 m/s$^{1.5}$. These results indicate that sinusoidal humps most effectively attenuate vibration dose at the front

child seat, with statistically significant but smaller improvements observed at the rear seat and frame. Notably, variability in VDV reduction at the frame was lower relative to peak acceleration analyses, indicating more consistent dose attenuation across scenarios.

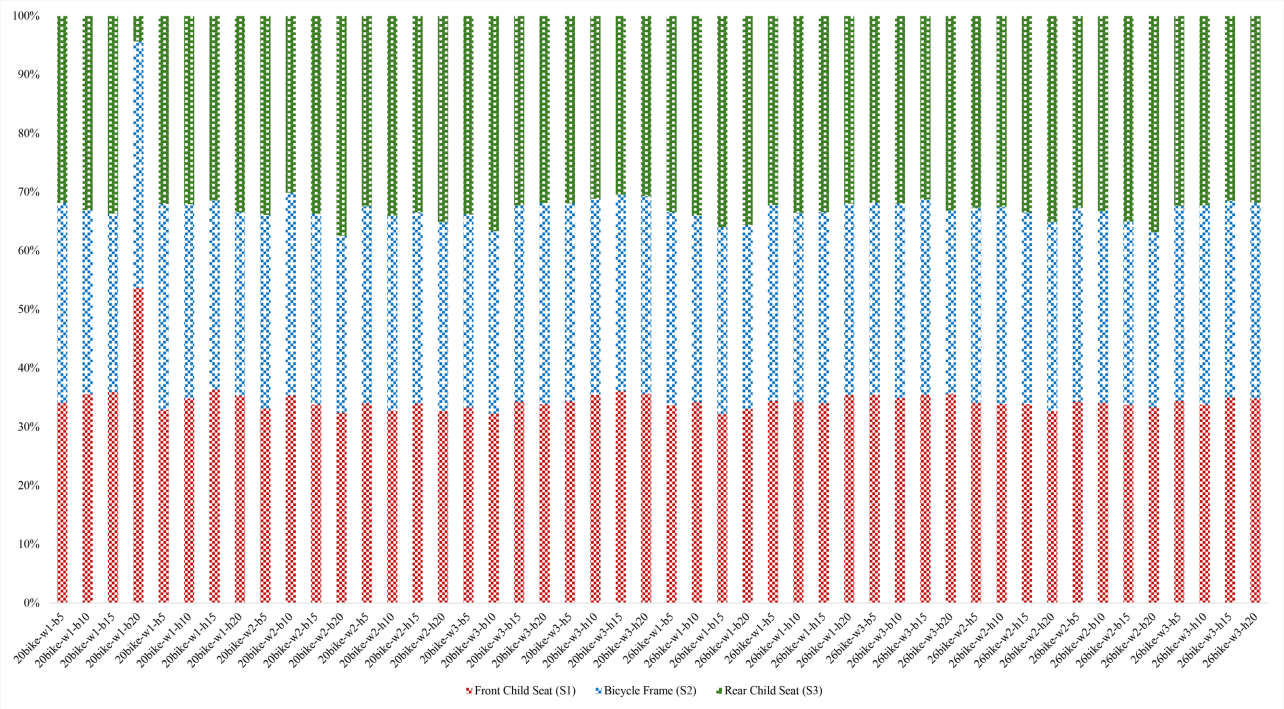

Figure 10. RMS variation over sensor location.

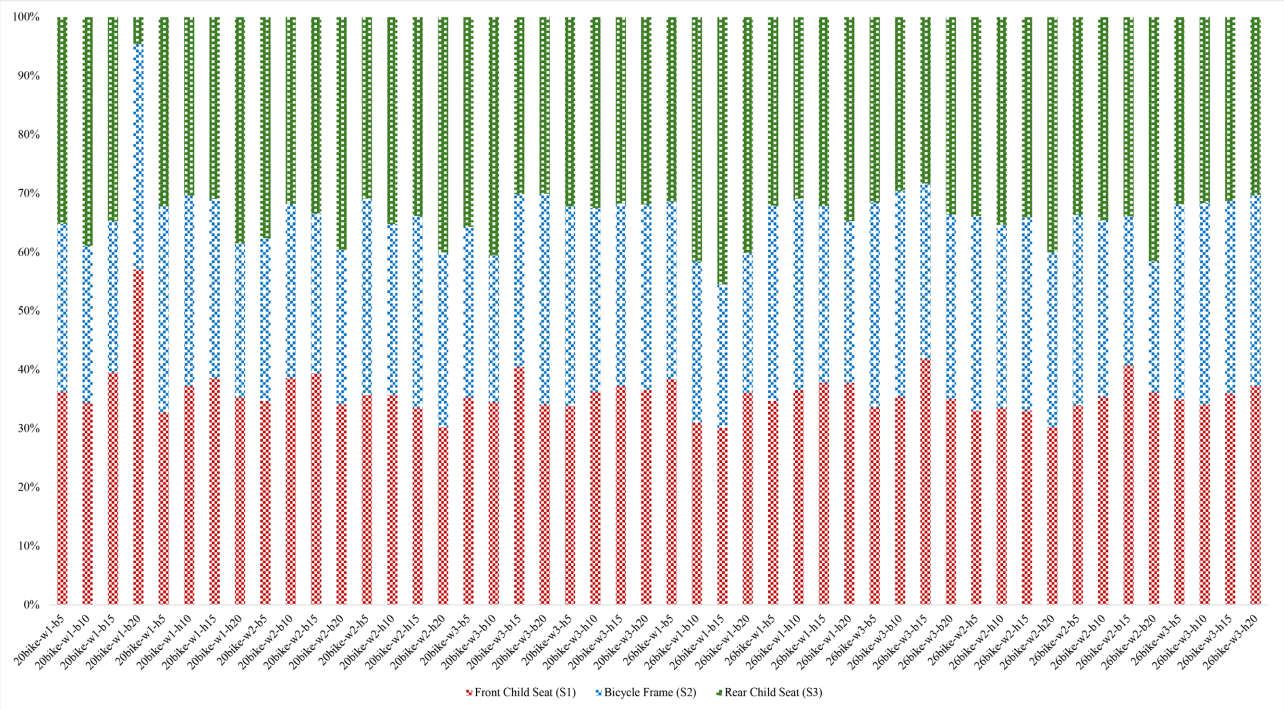

Figure 11. VDV variation over sensor location.

Analysis of crest factor reductions across sensor positions indicates the frame-mounted sensor (S2) experienced the smallest mean decrease of 1.65 under sinusoidal humps compared to bumps (mean hump = 2.10, mean bump = 3.75). In contrast, the front-seat sensor (S1) and rear-seat sensor (S3) exhibited larger mean reductions of 2.05 (mean hump = 2.83, mean bump = 4.88) and 2.10 (mean hump = 2.84, mean bump = 4.94), respectively, demonstrating that sinusoidal profiles provide the greatest reduction in crest factor at the child seat locations while still significantly benefiting the bicycle frame as shown in Figure 12.

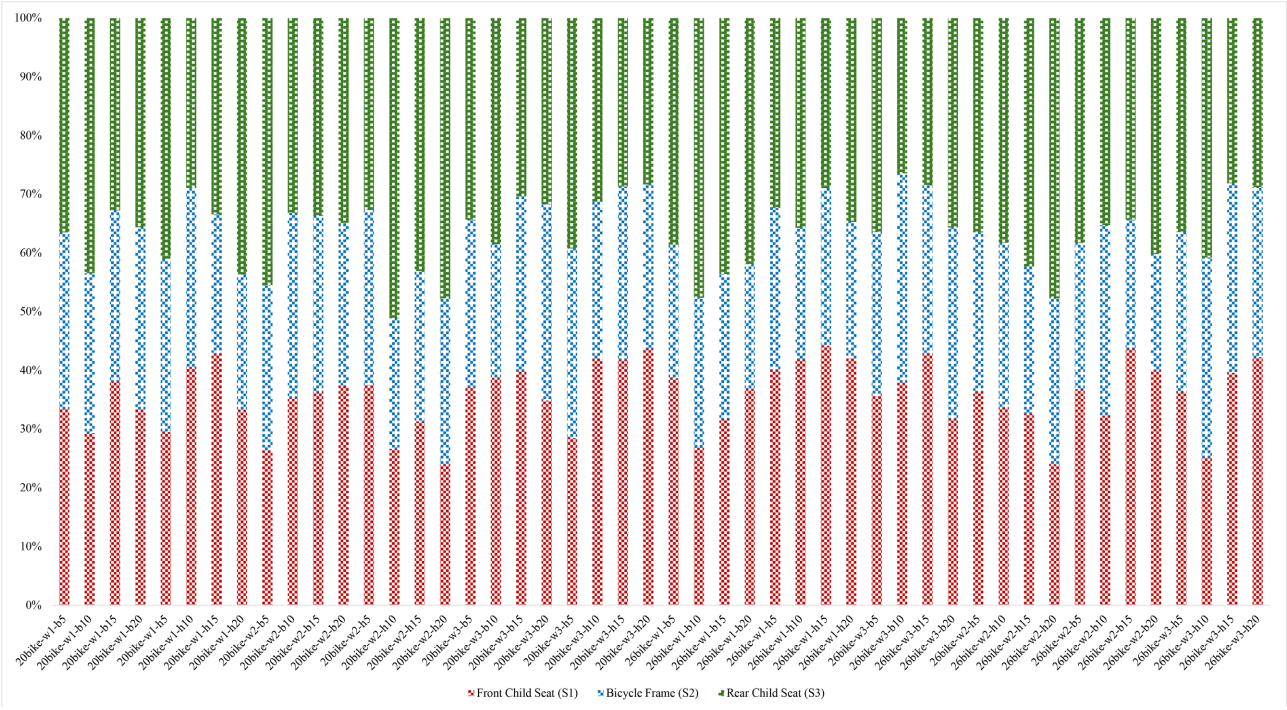

Figure 12. Crest Factor variation over sensor location.

Across all comfort and health metrics, sinusoidal speed humps consistently outperformed conventional bumps in attenuating vibrations transmitted to the bicycle and child seats. The front child seat benefited most, exhibiting the greatest reduction in abrupt jolts, overall vibration, cumulative dose, and peak-to-average ratios, thereby offering the highest comfort gain. The rear child seat also showed substantial improvements across all metrics, while the bicycle frame experienced notable but slightly smaller reductions. Table 3 outlines statistical comparison for comfort and health metrics.

6.3. Biomechanical Implications for Child Passenger Safety

The observed reductions in peak acceleration, RMS vibration, and vibration dose value at child seat locations carry important implications for infant passenger safety on electric-assisted child-carrying bicycles. Previous research has identified dominant vibration frequencies in the 3 - 5 Hz range during bicycle transport, which coincide with infant head resonance frequencies and may amplify discomfort. The

Table 3. Summary of paired comparisons.

Metric	Statistic Test Results				
	Mean (Hump)	Mean (Bump)	t-stat	p-value (t-test)	Wilcoxon p-value
RMS	10.62	11.70	−5.39	8.69×10^{-7}	4.03×10^{-12}
VDV	24.09	32.50	−7.61	8.64×10^{-11}	3.78×10^{-10}
Peak a	27.95	54.11	−11.51	6.71×10^{-18}	2.71×10^{-12}
Crest Factor	2.59	4.52	−14.30	1.35×10^{-22}	1.88×10^{-13}

study's findings demonstrate that sinusoidal humps reduce peak vertical accelerations at the front child seat (S1) by a mean of 29.29 m/s^2 compared to conventional bumps. This attenuation is significant given that biomechanical testing has identified critical frequencies of 1 - 2 Hz where infant head and chest regions exhibit peak vibrational responses, indicating potential resonance amplification during cycling operations. The substantial reduction in VDV at the front child seat 10.73 $m/s^{1.5}$ directly addresses concerns regarding cumulative vibration exposure to developing pediatric structures. While cycling vibration magnitudes remain well below injury thresholds for abusive head trauma, the sinusoidal hump design's demonstrated ability to maintain VDV values within acceptable comfort thresholds even at electric-assist speeds (20 - 25 km/h) provides a safety margin against potential cumulative effects. The reduction in Crest Factor at child seat positions (mean reduction of 2.05 - 2.10) when traversing sinusoidal humps indicates substantial mitigation of impulsive shock events. This is particularly relevant to infant passengers, whose reduced tissue mass may increase vibration transmissibility to sensitive anatomical structures. By attenuating these shock components, sinusoidal profiles reduce mechanical stress imposed on infant passengers while maintaining effective speed control functionality.

6.4. Study Limitations and Future Research Directions

This study provides quantitative evidence supporting sinusoidal speed hump implementation for child-carrying bicycles; however, several methodological limitations warrant acknowledgment. The experiment employed 12 kg static weights rather than pediatric Anthropomorphic Test Devices (ATDs), which cannot replicate dynamic coupling between seat vibration and infant body resonances. Vertical acceleration analysis dominated; however, multi-directional loading during hump traversal may contribute to overall exposure. Testing was conducted by a single rider, limiting generalizability to diverse populations with varying postures and body mass distributions, though this approach eliminated inter-individual variation and improved consistency. The study examined four discrete speeds (5, 10, 15, 20 km/h) and two-wheel sizes at three loading conditions but did not investigate tire pressure or alternative seat mounting configurations. Additionally, single-hump traversal does not capture cumulative vibration dose effects when

cyclists encounter multiple sequential humps in practical Zone 30+ implementations.

Despite these limitations, the controlled experimental design provides robust comparative evidence for sinusoidal hump superiority across 144 scenarios. Future research should employ age-appropriate pediatric ATDs, incorporate multi-axis ISO 2631-1 metrics, expand the rider population matrix, evaluate multi-hump sequences, and integrate findings with pediatric biodynamic models to establish comprehensive safety guidelines for emerging traffic calming technologies in Japanese residential environments.

7. Conclusions

This study demonstrates that sinusoidal speed humps provide significantly superior comfort characteristics compared to conventional speed bumps for electric-assisted child-carrying bicycles in Japanese Zone 30+ environments. Through comprehensive evaluation of 144 experimental scenarios encompassing diverse wheel sizes, loading conditions, speeds, and sensor locations, the research establishes empirical evidence supporting the implementation of sinusoidal traffic calming infrastructure in residential areas where vulnerable road users require protection.

The Dynamic Comfort Index analysis reveals that sinusoidal humps consistently yield higher DCI values across both 20-inch and 26-inch wheel configurations ($p < 0.000001$), indicating reduced vibration exposure and enhanced passenger comfort. The bicycle frame emerges as the optimal location for vibration attenuation, while systematic assessment of ISO 2631-1 metrics demonstrates that sinusoidal profiles maintain acceptable comfort thresholds whereas conventional bumps frequently exceed uncomfortable limits, particularly at elevated speeds typical of electric-assisted operation. Spatial analysis of sensor locations confirms that front child seats experience the greatest comfort benefits from sinusoidal humps, with mean reductions of 29.29 m/s^2 in peak acceleration, 1.25 m/s^2 in RMS acceleration, and 10.73 $m/s^{1.5}$ in vibration dose value compared to conventional bumps. These findings are particularly significant given that electric-assisted bicycles operate at sustained speeds of 20 - 25 km/h, substantially higher than conventional bicycle velocities, thereby amplifying the importance of vibration mitigation for child passenger safety and comfort.

This research provides quantitative foundations for evidence-based traffic calming policy in Japanese municipalities expanding Zone 30+ implementations. The demonstrated superiority of sinusoidal geometry in minimizing impulsive accelerations while maintaining effective speed reduction capabilities supports their widespread adoption in school zones and residential streets. Furthermore, the study's systematic characterization of wheel size effects, loading conditions, and velocity dependencies offers critical insights for bicycle manufacturers, infrastructure designers, and urban planners seeking to optimize sustainable family transportation systems.

Acknowledgements

The field experiment survey was implemented with financial support from Saitama University. The authors also sincerely thank all stakeholders (Nippon Liner Co., Ltd.) for their enthusiasm and support for this research study.

Conflicts of Interest

The authors declare no conflicts of interest regarding the publication of this paper.

References

[1] Rothhämel, M. (2023) Measuring Vertical Tyre Stiffness of Bicycle Tyres. *Bicycle and Motorcycle Dynamics* 2023: *Symposium on the Dynamics and Control of Single-Track Vehicles*, Delft, 18-20 October 2023, 8. https://doi.org/10.59490/650c004def25b2f0766f520b

[2] Du, W., Zhang, D. and Zhao, X. (2009) Research on Battery to Ride Comfort of Electric Bicycle Based on Multi-Body Dynamics Theory. 2009 *IEEE International Conference on Automation and Logistics*, Shenyang, 5-7 August 2009, 1722-1726. https://doi.org/10.1109/ical.2009.5262700

[3] Kojima, A., Kubota, H., Yoshida, M., Ichihara, S. and Yoshida, S. (2011) Effectiveness of Speed Humps Ranged at Different Intervals Considering Roadside Environment Including Vehicle Speed, Noise and Vibration. *Journal of the Eastern Asia Society for Transportation Studies*, **9**, 1913-1924. https://doi.org/10.11175/easts.9.1913

[4] Giacomin, J.A. (2003) An Experimental Investigation of the Vibrational Comfort of Child Safety Seats. Master's Thesis, University of Sheffield.

[5] Nabizada, M., Kojima, A. and Kubota, H. (2024) Assessment of Effectiveness of Different Speed Hump Shapes on the Car Vibration Using Computer Simulation. *Journal of the Eastern Asia Society for Transportation Studies*, **15**, 2729-2745. https://doi.org/10.11175/easts.15.2729

[6] Rothhämel, M. (2023) Comfort and Vibration Level of Children in Cycle Carriers. *PLOS ONE*, **18**, e0282778. https://doi.org/10.1371/journal.pone.0282778

[7] Martial, L., Nakamura, F. and Miura, S. (2019) Bicycle Success by Social Acceptance: The Example of Japan. *Proceedings of the International Alliance for Sustainable Urbanization and Regeneration*, Xi'an, 29-31 March 2019, 8.

[8] Inada, H., Tomio, J., Nakahara, S. and Ichikawa, M. (2020) Area-Wide Traffic-Calming Zone 30 Policy of Japan and Incidence of Road Traffic Injuries among Cyclists and Pedestrians. *American Journal of Public Health*, **110**, 237-243. https://doi.org/10.2105/ajph.2019.305404

[9] Mimura, Y. and Yamaoka, S. (2024) Maintenance Trends for Traffic Calming Devices in Zone 30 Plus. *Journal of the City Planning Institute of Japan*, **59**, 1706-1713. https://doi.org/10.11361/journalcpij.59.1706

[10] Webster, D.C. and Layfield, R.E. (1998) Traffic Calming: Sinusoidal, "H" and "S" Humps. Transport Research Laboratory. https://www.trl.co.uk/uploads/trl/documents/TRL377.pdf

[11] Steele, M.W. (2010) The Speedy Feet of the Nation: Bicycles and Everyday Mobility in Modern Japan. *The Journal of Transport History*, **31**, 182-209. https://doi.org/10.7227/tjth.31.2.5

[12] Bíl, M., Andrášik, R. and Kubeček, J. (2015) How Comfortable Are Your Cycling Tracks? A New Method for Objective Bicycle Vibration Measurement. *Transporta-*

tion Research Part C: *Emerging Technologies*, **56**, 415-425. https://doi.org/10.1016/j.trc.2015.05.007

[13] Vasudevan, V., Rajurkar, A., Soni, R. and Tiwari, A. (2018) Design and Evaluation of K-Pass: A Bicycle-Friendly Modification of Speed Bumps. *Transportation Research Record*: *Journal of the Transportation Research Board*, **2672**, 157-166. https://doi.org/10.1177/0361198118783171

[14] Gheibollahi, H. and Masih-Tehrani, M. (2021) Optimal Speed Control Humps Design Based on Driver Comfort. *International Journal of Automotive and Mechanical Engineering*, **18**, 8941-8958. https://doi.org/10.15282/ijame.18.3.2021.08.0685

[15] Kyrollos, D.G., Stachiw, T., Green, J.R. and Langlois, R.G. (2020) Injury Risk and Comfort Assessment Applied to Ambulance Transportation. *International Conference of Control*, *Dynamic Systems*, *and Robotics*, 23-25 November 2020, 156-1-156-10. https://doi.org/10.11159/cdsr20.156

[16] Rothhämel, M. and Liu, Y. (2024) On Comfort in Cycle Carriers for Child Transport. In: Huang, W. and Ahmadian, M., Eds., *Advances in Dynamics of Vehicles on Roads and Tracks III*, Springer, 792-801. https://doi.org/10.1007/978-3-031-66968-2_78

[17] Mohamed, A. and Bigazzi, A. (2019) Speed and Road Grade Dynamics of Urban Trips on Electric and Conventional Bicycles. *Transportmetrica B*: *Transport Dynamics*, **7**, 1467-1480. https://doi.org/10.1080/21680566.2019.1630691

[18] Scoz, R.D., Amorim, C.F., Espindola, T., Santiago, M., Mendes, J.J.B., Oliveira, P.R.D., *et al.* (2021) Discomfort, Pain and Fatigue Levels of 160 Cyclists after a Kinematic Bike-Fitting Method: An Experimental Study. *BMJ Open Sport & Exercise Medicine*, **7**, e001096. https://doi.org/10.1136/bmjsem-2021-001096

[19] Ahmed, T., Pirdavani, A., Wets, G. and Janssens, D. (2024) Evaluating Bicycle Path Roughness: A Comparative Study Using Smartphone and Smart Bicycle Light Sensors. *Sensors*, **24**, Article 7210. https://doi.org/10.3390/s24227210